ORIGINAL ARTICLE

3D Printing of Anisotropic Bone-Mimetic Structure with Controlled Fluid Flow Stimuli for Osteocytes: Flow Orientation Determines the Elongation of Dendrites

Aira Matsugaki[1], Tadaaki Matsuzaka[1], Ami Murakami[1], Pan Wang[2], Takayoshi Nakano[1]*

[1]Division of Materials and Manufacturing Science, Graduate School of Engineering, Osaka University, 2-1 Yamada-oka, Suita, Osaka 565-0871, Japan

[2]Singapore Institute of Manufacturing Technology, 73 Nanyang Drive, 637662, Singapore

Abstract: Although three-dimensional (3D) bioprinting techniques enable the construction of various living tissues and organs, the generation of bone-like oriented microstructures with anisotropic texture remains a challenge. Inside the mineralized bone matrix, osteocytes play mechanosensing roles in an ordered manner with a well-developed lacunar-canaliculi system. Therefore, control of cellular arrangement and dendritic processes is indispensable for construction of artificially controlled 3D bone-mimetic architecture. Herein, we propose an innovative methodology to induce controlled arrangement of osteocyte dendritic processes using the laminated layer method of oriented collagen sheets, combined with a custom-made fluid flow stimuli system. Osteocyte dendritic processes showed elongation depending on the competitive directional relationship between flow and substrate. To the best of our knowledge, this study is the first to report the successful construction of the anisotropic bone-mimetic microstructure and further demonstrate that the dendritic process formation in osteocytes can be controlled with selective fluid flow stimuli, specifically by regulating focal adhesion. Our results demonstrate how osteocytes adapt to mechanical stimuli by optimizing the anisotropic maturation of dendritic cell processes.

Keywords: Bioprinting, Collagen substrate, Mineralization, Osteocyte, 3D arrangement of bone matrix

***Corresponding Author:** Takayoshi Nakano, Graduate School of Engineering, Osaka University, Osaka, Japan; nakano@mat.eng.osaka-u.ac.jp

Received: June 03, 2020; ***Accepted:*** June 25, 2020; ***Published Online:*** July 27, 2020

Citation: Matsugaki A, Matsuzaka T, Murakami A, *et al*., 2020, 3D Printing of Anisotropic Bone-Mimetic Structure with Controlled Fluid Flow Stimuli for Osteocytes: Flow Orientation Determines the Elongation of Dendrites, *Int J Bioprint*, 6(4): 293. DOI: 10.18063/ijb.v6i4.293

1 Introduction

The highly ordered three-dimensional (3D) microstructured bone matrix determines the specialized anisotropic bone function[1]; for example, the collagen/apatite bone matrix shows anisotropic texture depending on the anatomical position, which realizes the mechanoadaptation of bone tissue[2-4]. Although several approaches have been made for the development of bone-mimetic structures *in vitro*[5-7], conventional monolayered two-dimensional (2D) cultures have limitations in approaching the crosstalk among multiple cell types in biomimetic niches. Development of an appropriate 3D platform is critical for the manufacturing of a functional bone tissue equivalent since a 3D environment is necessary for bone cell functionalization. In particular, osteocytes are embedded in the mineralized matrix with an ordered cell arrangement, surrounded by a networked lacunar-canaliculi system[8]. Increasing evidence shows that osteocytes play

crucial roles in bone metabolism in response to the mechanical environment[9,10]. The cellular activities of osteocytes are regulated by the fluid flow inside canaliculi, which is primarily caused by compressive loading of the bone related to physical activity. Therefore, control of the anisotropic bone matrix microstructure and fluid flow stimuli must be established in 3D bone-mimetic constructs for understanding the relationship between osteocyte mechanosensation and bone tissue architecture.

3D bioprinting techniques represent an additive manufacturing technology for developing living tissues or organs[11]. Bioprinting procedures are mainly classified into three categories: extrusion[12], jetting[13,14], and vat polymerization techniques[15]. These procedures allow the positional control of cells throughout the cultivation period. Spatiotemporally controlled deposition of living cells and biomaterials is required for the establishment of the biomimetic construct; in this context, placement of each cell at the proper position under controlled cell maturation conditions is expected. Importantly, osteocytes are pivotal cells for the mechanical functionalization of bone tissue, and their function cannot be achieved without the 3D surrounding matrix environment[16]. We previously developed a 2D biofabrication method for controlling the ordered arrangement of osteoblasts using the extrusion method of collagen molecules[17]. While our work has revealed that monolayered control of osteoblast alignment is efficient for the development of oriented collagen/apatite matrix deposition[17-19], control of bone matrix-embedded osteocytes is hard to achieve in 2D culture; therefore, bone cell culture in a 3D niche is necessary for the spatiotemporal control of the bone-mimic structure.

In this study, an innovative method combining collagen extrusion and sheet lamination was developed. Furthermore, the functional responses of osteocytes to mechanical stimuli were addressed by providing directional fluid flow in parallel or perpendicular to the substrate 3D orientation.

2 Materials and methods

2.1 Fabrication of the 3D oriented collagen scaffold

3D oriented collagen substrates were produced by combining the sheet lamination (ASTM F2792) and hydrodynamic extraction methods[17]. Collagen solution (10 mg/mL in 0.02 N acetic acid, pepsin-solubilized collagen type-I derived from porcine skin (Nippi)) was deposited into phosphate buffer saline (PBS) solution under control with a three-axis robotic arm (Musashi Engineering), which could regulate the orientation and degree of orientation of collagen fibers (**Figure 1A**). Two types of 3D collagen scaffold ("random" and "oriented") were built using lamination method with control of a robotic arm in 3D directions. The collagen scaffold without preferred orientation was fabricated by controlled lamination of isotropic collagen sheets produced by deposition of type I collagen solution onto the flat field. The 3D scaffolds were soaked in PBS to obtain sufficient swelling.

2.2 Ethics statement

The Osaka University Committee for Animal Experimentation approved all the animal experiments (approval number: 27-2-1). The authors performed all experiments in accordance with the related guidelines for ethical and scientific animal experimentation.

2.3 Primary culture of mouse osteoblast

We isolated primary osteoblasts from the neonatal mice calvariae using sequential enzymatic protocol[20]. Calvariae were extracted from neonatal C57BL/6 mice in cold α-minimal essential medium (MEM) (Thermo Fisher Scientific), and the surrounding tissues and cells around the bone were cleanly eliminated. The extracted calvariae tissue was digested with collagenase (Wako)/trypsin (Nacalai Tesque). The digestion procedure was repeated five times at 37°C for 15 min each after the tissue was finely cut and washed with Hank's balanced salt solution (HBSS). After centrifugation of the first two

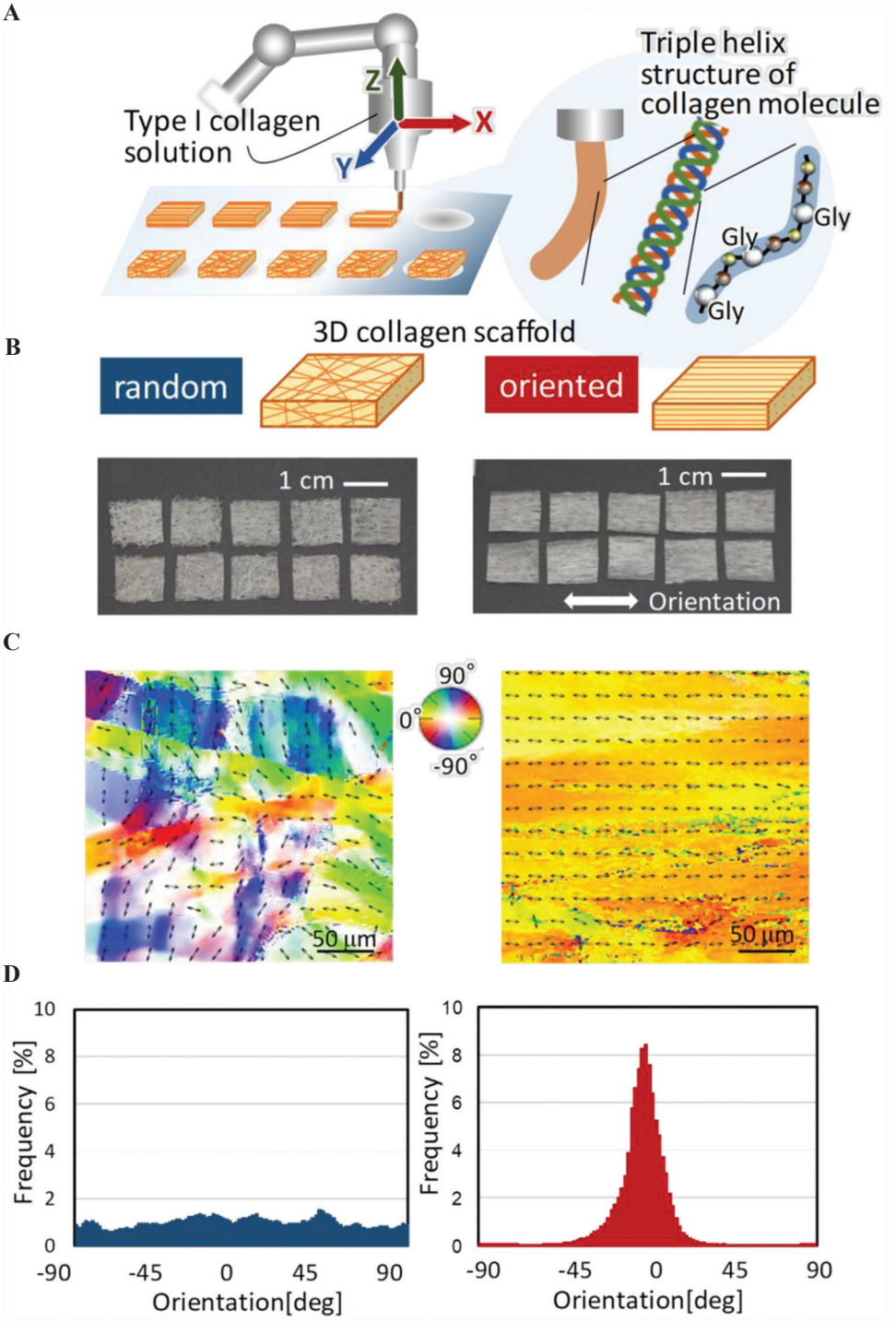

Figure 1. Fabrication of three-dimensional (3D) oriented collagen scaffolds with controlled molecular alignment. (A) Type I collagen solution was deposited with a controlled 3D robotic arm. Collagen solution was extruded from the nozzle, allowing fibril formation with aligned molecular arrangement of amino acid sequencing (Gly-X-Y). Each oriented collagen fiber sheet was laminated layer by layer for 3D construct. (B) Appearance of the fabricated 3D collagen substrates. Left; scaffold with random orientation. Right; one-directional oriented scaffold. (C) Birefringence analysis of the substrates. The bidirectional arrows and color maps show the orientation of collagen fiber in the obtained scaffold. (D) The angular distribution of the collagen fiber orientation in the scaffold determined from the corresponding birefringence images.

treatments, the supernatants were disposed. The obtained supernatants involving from the third to fifth treatments were collected in α-MEM. We filtrated the collections through a cell strainer (BD Biosciences), centrifuged, and the supernatant was removed. The extracted cells were resuspended in α-MEM containing 10% fetal bovine serum, penicillin/streptomycin (Thermo Fisher Scientific) for cell culture. The obtained cells were then plated into the fabricated specimens at a density of 2.0×10^4 cells per mL. The media were changed twice weekly, and after culturing for 1 week, the media were supplemented to reach final concentrations of 10 mM β-glycerophosphate (Tokyo Kasei), 50 μg/mL ascorbic acid (Sigma-Aldrich), and 50 nM dexamethasone (MP Bioscience).

2.4 Primary culture of osteocyte

We isolated primary osteocytes from mature murine femurs, humeri, and tibiae based on a sequential digestion method[21]. Long bones were excised from mature C57BL/6 mice in fresh α-MEM (Thermo Fisher Scientific) with penicillin/streptomycin. The surrounding tissues around the bone were eliminated. The obtained bone specimens were then cut into fraction of 1–2 mm in length and cleaned in HBSS. The pieces were exposed to total nine repeated cycles of enzymatic digestion procedure for 25 min at 37°C each step. During the first three digestions, we incubated the bone fragments with collagenase (Wako) solution followed by cleaning in HBSS thrice. From the fourth treatment, we incubated the bone fragments in collagenase and ethylenediaminetetraacetic acid in turns and cleaned in HBSS thrice. Following that, the treated bone fragments were cut and immersed in α-MEM with penicillin/streptomycin and 10% fetal bovine serum. Osteocyte-like cells were obtained from migrated cells from the cultured bone chips after 7–10 days. Isolated cells were plated into the fabricated 3D substrates at a diluted density of 1×10^5 cells/mL.

2.5 Fluid flow stimulation

The cell-seeded 3D scaffolds were inserted into custom-made flow chambers for fluid flow stimulation with a peak shear stress of 80 dyn/cm^2 for 4 h. Static control cells were also inserted into the flow chambers without flow stimulation. The applied shear stress was calculated based on the Hagen–Poiseuille equation:

$$\tau_w = {4Q\mu}/{\pi R^3} \quad (1)$$

Where, τ_w is the fluid shear stress, Q is the volumetric flow rate, R is the radius of tubing, approximating the flow channel as the same number of collagen fiber strings, and μ is the viscosity coefficient of the culture medium. To apply the Hagen–Poiseuille equation, the following conditions were satisfied: Steady-state laminar flow, inelastic tubing, and Newtonian fluid of culture medium.

2.6 Analysis of substrate collagen orientation

The collagen orientation in the fabricated scaffold was assessed using a birefringence measurement system (WPA-micro, Photonic Lattice). The integrated polarizer allowed to detect the polarization axis with the greater index of refraction (slow axis). The average direction of the slow axis in collagen molecule corresponding to each pixel was analyzed using the equipped software (WPA-VIEW, Photonic Lattice).

2.7 Immunostaining

The cells were fixed with paraformaldehyde and then washed with PBST (PBS-Triton X100) containing normal goat serum (Thermo Fisher Scientific) for 30 min to avoid non-specific binding of antibodies. We incubated the fixed cells with primary antibodies against Sclerostin (Abcam) or Src (Cell Signaling) at 4°C for half a day. After rinsing with PBST, we applied secondary antibodies (Alexa Fluor 546 Immunoglobulin G, Thermo Fisher Scientific) and DAPI (Thermo Fisher Scientific) at room temperature for 2 h. For visualization of F-actin, the cells were incubated with Alexa Fluor 488 phalloidin (Thermo Fisher Scientific). Finally, the stained cells were washed in PBST, followed by mounting using Antifade Reagent (Prolong Gold, Thermo Fisher Scientific). Fluorescent images were obtained under a confocal microscope (FV1000D-IX81, Olympus)

and processed using the Adobe Photoshop 10.0 software. For quantitative analysis of dendritic cell processes, dendrites with length of more than 20 μm were counted[22]. The angle of cell processes was analyzed as a reference of substrate collagen orientation.

2.8 Gene expression analysis

We extracted total RNA from the cultured cells using column method (NucleoSpin RNA XS, Macherey-Nagel). The expression levels of Src gene were assessed with quantitative polymerase chain reaction (PCR) according to the manufacturer's guidelines (Applied Biosystems). The Ct value was set within the exponential stage in the PCR. The expression level for each target gene was determined by standardization of the expression value of *Gapdh*. We provide the obtained results as the gene expression (percentage) relative to *Gapdh* expression and then normalized to parallel group.

2.9 Crystallographic texture of the bone matrix

We analyzed the characterization of apatite crystals and their preferred *c*-axis orientation produced by osteoblasts using a microbeam X-ray diffraction system with Mo-Kα radiation (R-Axis BQ; Rigaku) at 50 kV and 90 mA[23]. The specimens were fixed in 10% formaldehyde for analysis. The preferred orientation of the apatite *c*-axis was evaluated. The relative integrated intensity ratio of the (002) diffraction peak to the (310) peak was calculated based on the measurement along the longitudinal axis and transverse direction of the specimens.

2.10 Statistical analysis

Statistical significance was assessed by one-way ANOVA, followed by Tukey's *post hoc* test. A significance of $P < 0.05$ was required for rejecting the null hypothesis.

3 Results

3.1 Fabrication of 3D oriented collagen scaffold with controlled molecular alignment

A 3D oriented microstructured collagen scaffold was successfully produced by an extrusion-based method combined with controlled lamination of each sheet (**Figure 1B**). Birefringence analysis of the fabricated substrates revealed that the control scaffolds showed no preferred alignment of collagen fibers, whereas unidirectional controlled extrusion allowed a uniformly aligned microstructure in one direction (**Figure 1C**). Quantitative analysis of the slow axis of collagen molecules (corresponding to the long axis of collagen fiber) exhibited random and unidirectional angular distribution of collagen fibers in the control and oriented substrates, respectively (**Figure 1D**).

3.2 Anisotropic bone matrix formation by 3D culture of primary osteoblasts

Primary osteoblast cells isolated from neonatal mice calvariae were cultured within the fabricated 3D oriented collagen substrates for 4 weeks in an osteoinductive environment (**Figure 2A**). Osteoblasts showed proliferative and differentiation activities inside the substrates with well-mineralized bone matrix formation. Cells embedded in the substrates showed Sclerostin-positive osteocyte-like morphology (**Figure 2B and C**). The mineralized bone matrix produced by the aligned osteoblasts presented a well-characterized X-ray diffractometer profile for apatite crystals. The integrated intensity ratio of (002)/(310) corresponding to the preferred orientation of the *c*-axis of apatite crystals, showed a significantly higher level along the longitudinal direction in the substrate collagen orientation rather than the transverse orientation of the substrates (**Figure 2D**).

3.3 Osteocyte responses for fluid flow stimulation inside 3D collagen substrates

Primary osteocytes were successfully obtained from the bone fragments derived from the mature bone tissue (**Figure 3A**). Cells inside the bone chips migrated and adhered onto the cell culture plate, presenting typical morphology with multiple cell processes (**Figure 3B**). Isolated osteocytes cultured inside the fabricated substrates were stimulated with controlled unidirectional

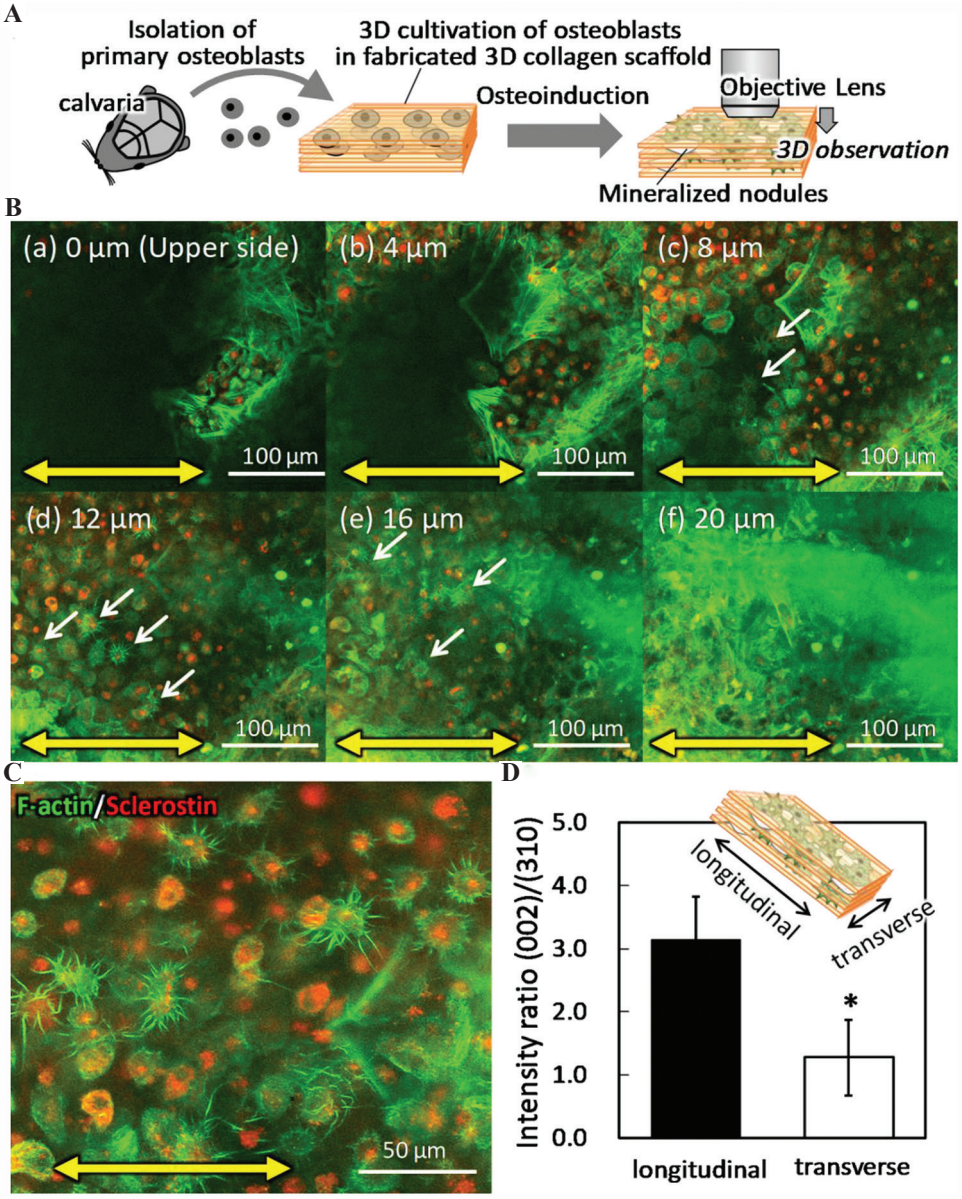

Figure 2. Anisotropic bone matrix formation in three-dimensional (3D) culture of primary osteoblasts. (A) Schematic illustration of the 3D culture procedure of primary osteoblasts. (B) Confocal microscopy analysis of immunofluorescent images of the cells inside the 3D mineralized matrix depending on the distance from the substrate surface. The substrate orientation is indicated by bidirectional yellow arrows. Arrows indicate the osteocyte-like cells with multiple dendritic processes. Green; F-actin, red; sclerostin. (C) Z-stacked immunocytochemical image of the cells inside the scaffold. Green; F-actin, red; sclerostin. (D) Microbeam X-ray diffraction analysis of the mineralized matrix. Bone matrix orientation was calculated with the intensity ratio of (002)/(310) in parallel and vertical direction to the substrate orientation. *: $P < 0.05$.

flow against the longitudinal direction of cell body, lacked cell processes along the substrate orientation, and generated the processes newly for the flow orientation (**Figure 3C**). Quantitative analysis of the cell process formation in the crossing direction against the substrate orientation showed significantly increased frequency in the vertical flow stimulated osteocytes (**Figure 3D**).

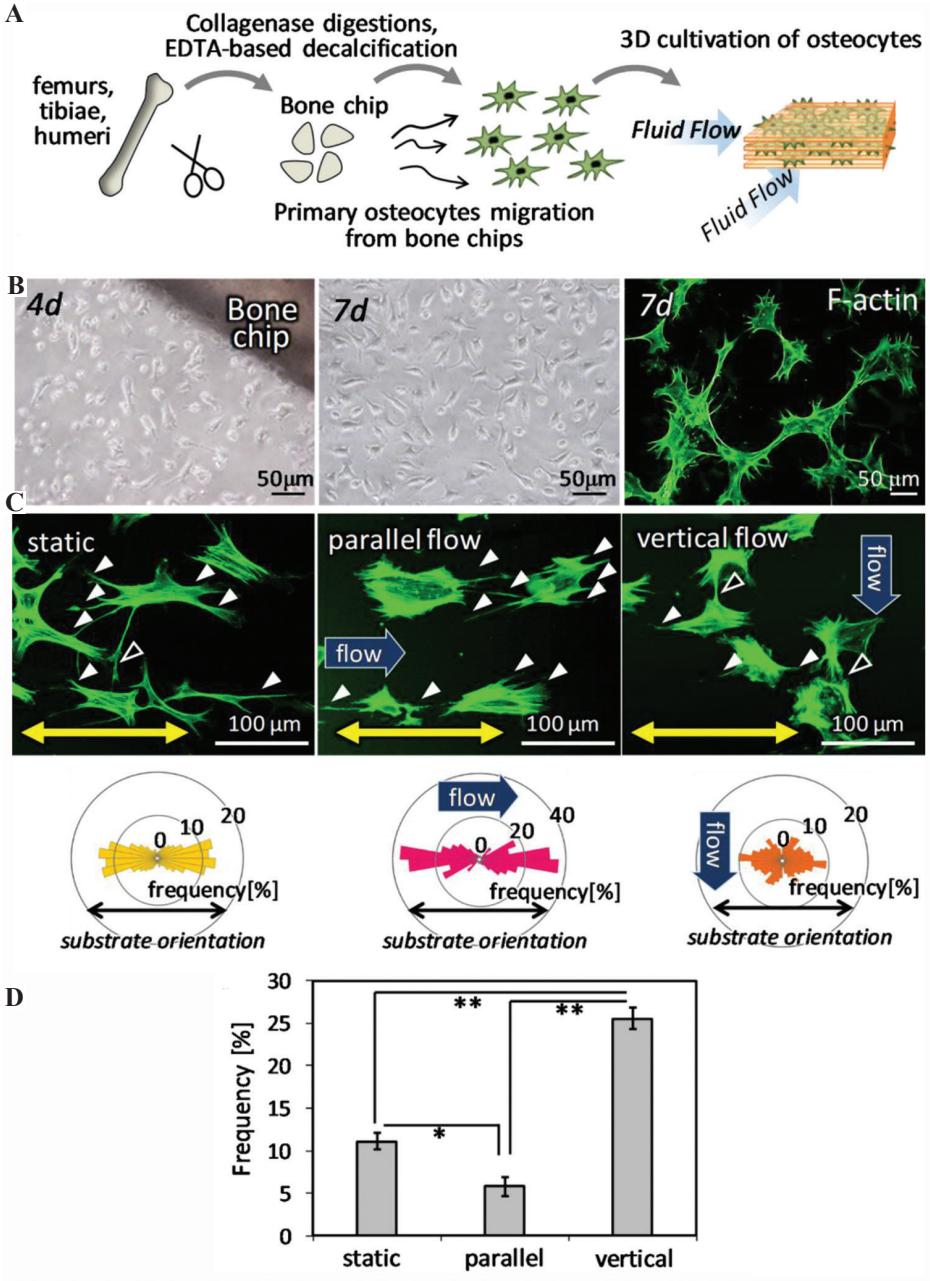

Figure 3. Osteocyte responses to the fluid flow stimulation inside three-dimensional (3D) collagen substrates. (A) Schematic illustration of 3D culture of primary osteocytes with controlled fluid flow stimuli. (B) Primary osteocyte-like cells migrated from the bone chips, with formation of mature dendritic cell processes. (C) Morphological change of osteocytes dendrites in response to the fluid flow direction. Green; F-actin. The directional distribution of the cell processes is shown below the corresponding images. (D) Appearance frequency of the cell process directing ± 30° from the vertical direction to substrate collagen orientation. *: $P < 0.05$, **: $P < 0.01$

3.4 Progressed expression of Src on stimulation with vertical fluid flow

Osteocytes exposed to the vertical flow had increased expression of the Src protein at the sites of elongated cell processes in the substrate orientation (**Figure 4A**). Gene expression analysis demonstrated significantly increased Src expression in the vertical flow-stimulated osteocytes (**Figure 4B**).

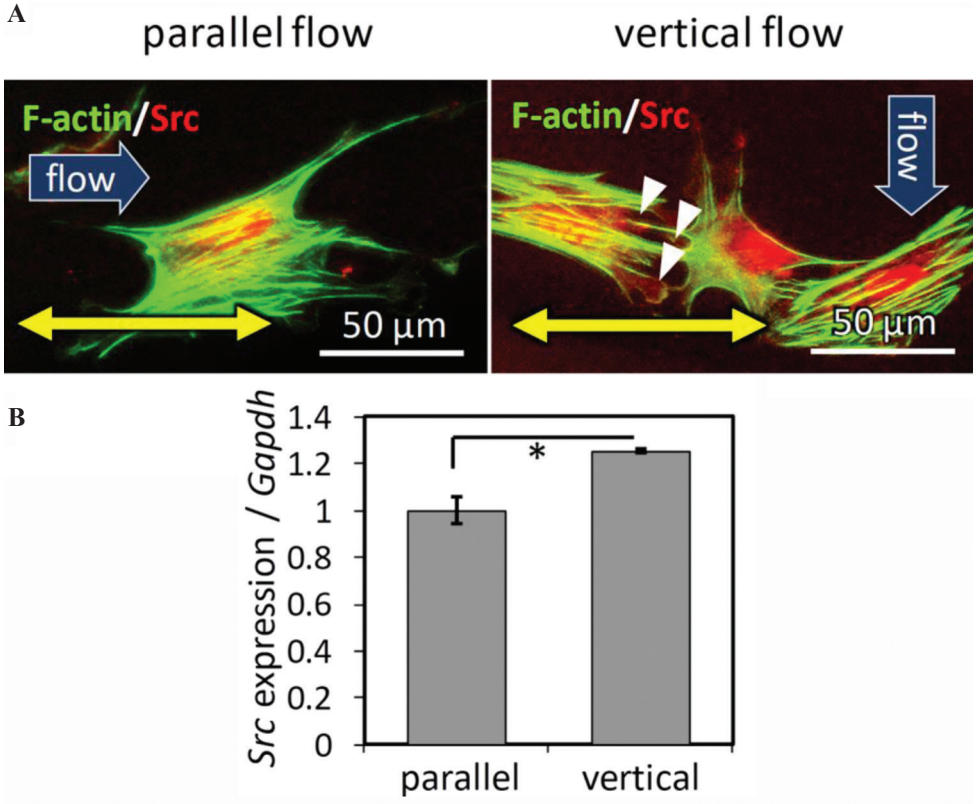

Figure 4. Src-mediated remodeling of osteocyte dendritic processes depending on the flow direction. (A) Immunocytochemical analysis of osteocytes under parallel and vertical flow. Arrowheads indicate the Src-positive focal adhesions. Green; F-actin, red; Src. Bidirectional arrows indicate the substrate collagen orientation. (B) Gene expression analysis of Src in osteocytes under parallel or vertical flow. *: $P < 0.05$.

These results indicate that the remodeling of cell processes is regulated by the reassembly of focal adhesion constructs mediated by Src expression.

4 Discussion

Engineering structurally organized 3D bone matrix constructs mimicking living bone tissue has great potential to accelerate the understanding of the cellular activities controlling various bone functions. In particular, the 3D arrangement of bone matrix and cellular components is essential for bone functionalization[24,25]. While traditional monolayer 2D cell culture systems provide a simple model of cell-cell interaction, 3D culture with biomimetic microstructure allows the artificial assembly of cellular networks and control of environmental factors[26]. In the present study, artificial 3D culture of osteocytes with preferred alignment of collagen scaffolds established the directional control of osteocyte orientation embedded inside the collagen substrates and revealed the mechano-induced remodeling of cell process generation by focal adhesion molecules.

Our novel 3D culture system provides freely controllable oriented collagen matrix scaffolds that show porosity enough for the migration and growth of cells inside the scaffold. It is noted that the cellular orientation mirrors the scaffold collagen orientation, leading to the construction of an anisotropic bone-like microstructured matrix (**Figure 2D**). The development of oriented bone matrix constructs is controlled by the interaction between aligned osteoblasts and scaffolds mediated by focal adhesion molecules[18,19]. The scaffold showed a diameter of approximately 50 μm for each collagen fiber, which is sufficient for cellular guidance through chemical interaction between collagen molecular orientation and cell receptors[27]. Our recent work revealed that

the bone matrix orientation can be controlled by operating the cellular arrangement even using a 2D material surface[28,29]. While the cell alignment inside the mineralized nodules is not clearly detected because of the confluency in cells, confocal microscopy analysis demonstrated that the cell population varies depending on the cellular positioning inside the scaffold. The top layer of long-term culture products of osteoblasts presented fibroblast-like cell morphology, whereas cells inside the 3D collagen scaffold expressed the mature osteocyte marker protein Sclerostin and adopted dendritic cell morphology (**Figure 2C**). The results obtained from confocal microscopic images revealed that 3D culture of osteoblasts using oriented collagen scaffold established the spatial control of cells which mimics the living bone system; osteoblasts on the bone surface, osteocytes embedded in the bone matrix they produced. The cellular connections in the stacking direction should be clarified and it will be reported in our next study. The results indicate that the fabricated 3D oriented scaffold can provide a successful matrix environment for the differentiation and maturation of osteocytes. Furthermore, the fabricated structure involving osteoblasts and their differentiated osteocytes can help the creation of mini-organ for the development of next-generation regenerative medicine. In particular, the developed 3D culture model can provide effective platforms for understanding the responses of osteocytes to mechanical stimuli.

Primary osteocytes were seeded and cultured inside the 3D collagen scaffold to realize fluid flow stimuli to individual cells. Osteocyte-like cells were successfully isolated from the bone fragments of mature long bones, with the formation of actin-rich dendrite structures typical for the osteocyte morphology embedded within the mineralized matrix. Under static conditions, osteocyte-like cells inside the oriented substrates showed elongated cell bodies along the collagen substrate orientation with the preferred alignment of the dendritic cell processes which are mainly parallel to the collagen substrate, with a few dendrites across the substrate orientation. The flow rate was determined based on the previous report of direct evaluation of solute movement in canaliculi[30]. We previously reported that the bone tissue microstructure is determined by controlling artificial stress applied to bone[31]. To provide a simulated condition of artificially controlled mechanical stimuli, the fluid stimuli was set as a higher level (80 dyn/cm^2) compared to the static physiological level. Although the fluid flow stimuli were strictly determined by the calculation as mentioned above, the pores and fibers could work as a barrier to disturb the fluid flow stimuli. The computational fluid dynamics simulation is now in progress to clarify the relationship between flow dynamics and cell responses.

Mechanical stimuli with a parallel flow to the collagen substrate promoted the dendrogenesis in the direction of fluid flow. This means that the normal parallel relationship between the direction of dendrite process and fluid flow generated the shear stress on the process surface, resulting in stimulation of dendrite growth. On the other hand, the flow stimuli across collagen orientation induced the degeneration of the dendrites elongated to the collagen orientation, stimulating the generation of dendritic cell processes parallel to the flow direction (**Figure 3C and D**). In addition, the extended flow stimulation could alter the morphological change of osteocyte cell body, as well as dendritic remodeling. The preferred formation of dendritic cell processes along flow stimuli direction, as opposed to under static condition, significantly demonstrated the role of fluid flow on the orientation of osteocytes dendritic processes. That is, the fluid flow stimuli rather than the substrate matrix orientation determine the direction of dendrites elongation.

Osteocyte dendrogenesis is now recognized to be controlled by biological signals in response to mechanical strain, meaning that osteocytes can actively regulate the formation of dendritic processes[22,32,33]. In particular, Src has been studied as an essential regulator in mechanotransduction mediating integrin-cytoskeleton interaction[34]. Here, we demonstrate the directional dendritic process remodeling of osteocytes in response to fluid flow shear stress mediated by Src expression (**Figure 4**). The quantitative gene expression

analysis revealed the upregulated expression of Src in vertical flow stimuli, whereas the expression in static condition will be investigated in our future study. Dendritic cell processes are anchored to the matrix wall through integrins, which experience fluid shear stress and transmit the mechanical stimuli into biochemical signals through multiple interactions with related proteins involving Src[35]. The upregulated expression of Src in vertical group means that the accelerated degradation of focal adhesion located in crossing direction to fluid flow was regulated accompanied with activated Src expression[36]. The obtained results indicate that osteocytes remodel dendritic cell processes to generate shear stress on their surface effectively under mechanical environmental stimuli. Our novel bioprinting technique allowed the establishment of bone-mimetic anisotropic 3D structure involving the desired arrangement of osteocytes inside the matrix, which are fully functionalized and surrounded with bone-like niche, compared to the traditional monolayer 2D culture system (**Figure 5**).

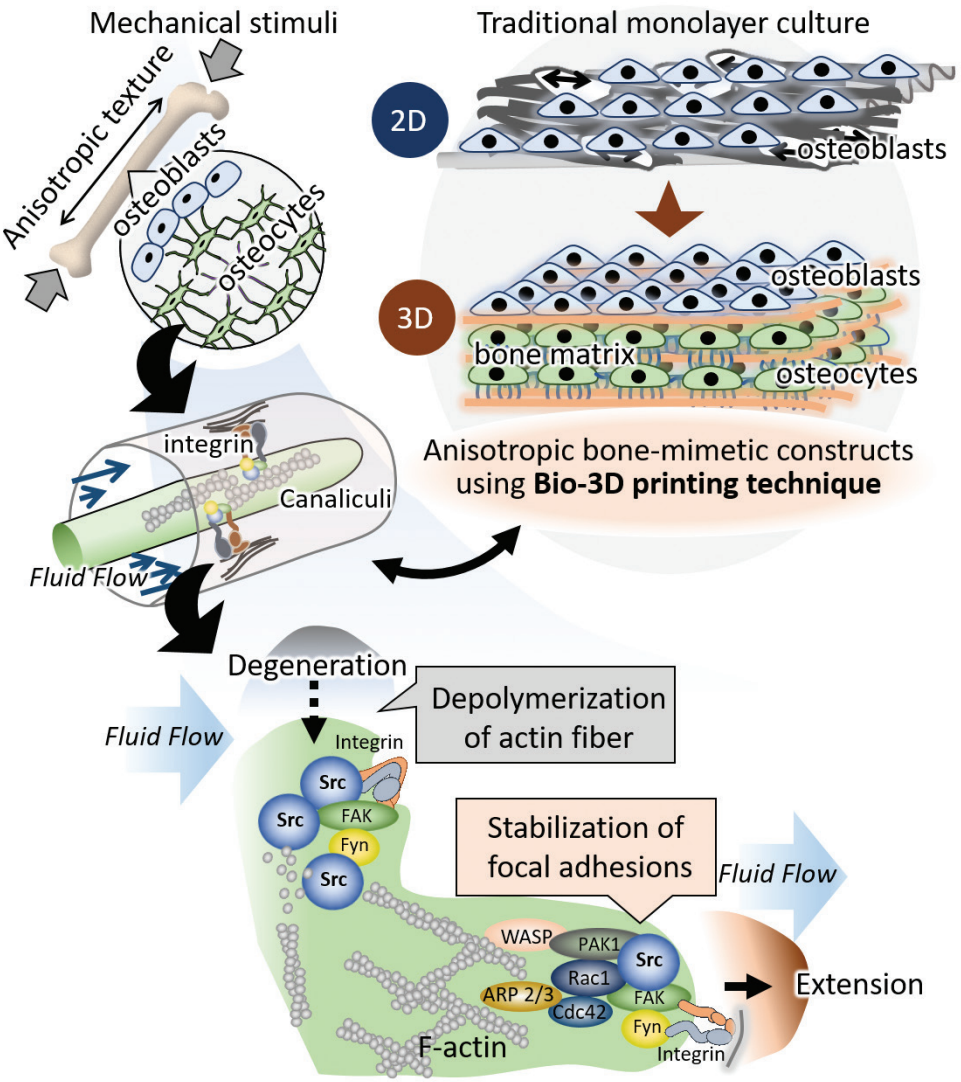

Figure 5. Novel bone-mimetic anisotropic three-dimensional (3D) construct fabricated with bio-3D printing technique. The obtained construct represents the 3D osteocytes networks which mimic the living bone tissue. Osteocytes remodel their dendritic processes to generate shear stress on their surface, resulting in the effective mechanosignaling.

5 Conclusion

A 3D bone-mimetic anisotropic microstructure was fabricated using the laminated layer method of oriented collagen sheets. Osteoblasts successfully constructed the aligned mineralized matrix with differentiation into mature osteocytes. The osteocytes embedded inside the scaffolds showed an ordered arrangement of the cell body as well as dendritic cell process, which remodeled their extrusion/degeneration depending on the flow direction. These findings indicate that functional adaptation of osteocytes in response to mechanical stimuli is regulated by the remodeling of cell processes mediated by Src expression in focal adhesions.

Acknowledgments

This research was funded by Grants-in-Aid for Scientific Research (S) (grant number 18H05254) and Grants-in-Aid for Scientific Research (A) (grant number 20H00308).

Conflicts of interest

The authors declare no conflicts of interest.

Authors' contributions

T. N. and A. MT. designed the study. T. M., A. MK., and A. MT. carried out the experiments. T. M., A. MT., P. W., and T. N. contributed to the interpretation of the results. A. MT. drafted the manuscript, P. W. and T. N. revised the manuscript content. All the authors contributed to the discussion of the results.

References

1. Ishimoto T, Nakano T, Umakoshi Y, *et al*., 2013, Degree of Biological Apatite c -axis Orientation Rather than Bone Mineral Density Controls Mechanical Function in Bone Regenerated Using Recombinant Bone Morphogenetic Protein-2. *J Bone Miner Res*, 28:1170–9. DOI: 10.1002/jbmr.1825.
2. Schaff F, Bech M, Zaslansky P, *et al.*, 2015, Six-dimensional Real and Reciprocal Space Small-angle X-ray Scattering Tomography. *Nature*, 527:353–6. DOI: 10.1038/nature16060.
3. Nakano T, Kaibara K, Tabata Y, *et al.*, 2002, Unique Alignment and Texture of Biological Apatite Crystallites in Typical Calcified Tissues Analyzed by Microbeam x-ray Diffractometer System. *Bone*, 31:479–87. DOI: 10.1016/s8756-3282(02)00850-5.
4. Nakano T, Kaibara K, Ishimoto T, *et al*., 2012, Biological Apatite (BAp) Crystallographic Orientation and Texture as a New Index for Assessing the Microstructure and Function of Bone Regenerated by Tissue Engineering. *Bone*, 51:741–7. DOI: 10.1016/j.bone.2012.07.003.
5. Hennessy KM, Pollot BE, Clem WC, *et al*., 2009, The Effect of Collagen I Mimetic Peptides on Mesenchymal Stem Cell Adhesion and Differentiation, and on Bone Formation at Hydroxyapatite Surfaces. *Biomaterials*, 30:1898–909. DOI: 10.1016/j.biomaterials.2008.12.053.
6. Lee S, Obata A, Brauer DS, *et al*., 2015, Dissolution Behavior and Cell Compatibility of Alkali-free MgO-CaO-SrO-TiO2-P2O5 Glasses for Biomedical Applications. *Biomed Glasses*, 1:151–8. DOI: 10.1515/bglass-2015-0015.
7. Prewitz MC, Seib FP, von Bonin M, *et al*., 2013, Tightly Anchored Tissue-mimetic Matrices as Instructive Stem Cell Microenvironments. *Nat Methods*, 10:788–794. DOI: 10.1038/nmeth.2523.
8. Bonewald LF, 2011, The Amazing Osteocyte. *J Bone Miner Res*, 26:229–38. DOI: 10.1002/jbmr.320.
9. Odagaki N, Ishihara Y, Wang Z, *et al*., 2018, Role of Osteocyte-PDL Crosstalk in Tooth Movement via SOST/Sclerostin. *J Dent Res*, 97:1374–82. DOI: 10.1177/0022034518771331.
10. Ganesh T, Laughrey LE, Niroobakhsh M, *et al*., 2020, Multiscale Finite Element Modeling of Mechanical Strains and Fluid Flow in Osteocyte Lacunocanalicular System. *Bone*, 2020:115328. DOI: 10.1016/j.bone.2020.115328.
11. Ng WL, Chua CK, Shen YF, 2016, Print Me An Organ! Why We Are Not There Yet. *Prog Polym Sci*, 2016:101145.
12. Ozbolat IT, Hospodiuk M, 2016, Current Advances and Future Perspectives in Extrusion-based Bioprinting. *Biomaterials*, 76:321–43. DOI: 10.1016/j.biomaterials.2015.10.076.
13. Gudapati H, Dey M, Ozbolat I, 2016, A Comprehensive Review on Droplet-based Bioprinting: Past, Present and Future, *Biomaterials*, 102:20–42. DOI: 10.1016/j.biomaterials.2016.06.012.
14. Ng WL, Lee JM, Yeong WY, *et al*., 2017, Microvalve-based Bioprinting Process, Bio-inks and Applications. *Biomater Sci*, 5:632–47. DOI: 10.1039/c6bm00861e.
15. Ng WL, Lee JM, Zhou M, *et al*., 2020, Vat Polymerization-based Bioprinting Process, Materials, Applications and Regulatory Challenges. *Biofabrication*, 12:22001. DOI:

10.1088/1758-5090/ab6034.

16. Wang K, Le L, Chun BM, *et al*., 2019, A Novel Osteogenic Cell Line that Differentiates into GFP-Tagged Osteocytes and Forms Mineral with a Bone-Like Lacunocanalicular Structure. *J Bone Miner Res*, 34:979–95. DOI: 10.1002/jbmr.3720.
17. Matsugaki A, Isobe Y, Saku T, *et al*., 2015, Quantitative Regulation of Bone-mimetic, Oriented Collagen/Apatite Matrix Structure Depends on the Degree of Osteoblast Alignment on Oriented Collagen Substrates: Anisotropic Construction of Cell-Produced Mineralized Matrix. *J Biomed Mater Res A*, 103:489–99. DOI: 10.1002/jbm.a.35189.
18. Nakanishi Y, Matsugaki A, Kawahara K, *et al*., 2019, Unique Arrangement of Bone Matrix Orthogonal to Osteoblast Alignment Controlled by Tspan11-Mediated Focal Adhesion Assembly. *Biomaterials*, 209:103–10. DOI: 10.1016/j.biomaterials.2019.04.016.
19. Kimura Y, Matsugaki A, Sekita A, *et al*., 2017, Alteration of Osteoblast Arrangement Via Direct Attack by Cancer Cells: New Insights into Bone Metastasis. *Sci Rep*, 7:44824. DOI: 10.1038/srep44824.
20. Wong G, Cohn DV, 1974, Separation of Parathyroid Hormone and Calcitonin-sensitive Cells from Non-responsive Bone Cells. *Nature*, 252:713–5. DOI: 10.1038/252713a0.
21. Stern AR, Stern MM, Van Dyke ME, *et al*., 2012, Isolation and Culture of Primary Osteocytes from the Long Bones of Skeletally Mature and Aged Mice. *Biotechniques*, 52:361–73. DOI: 10.2144/0000113876.
22. Matsugaki A, Yamazaki D, Nakano T, 2020, Selective Patterning of Netrin-1 as a Novel Guiding Cue for Anisotropic Dendrogenesis in Osteocytes. *Mater Sci Eng C*, 108:110391. DOI: 10.1016/j.msec.2019.110391.
23. Noyama Y, Nakano T, Ishimoto T, *et al*., 2013, Design and Optimization of the Oriented Groove on the Hip Implant Surface to Promote Bone Microstructure Integrity. *Bone*, 52:659–67. DOI: 10.1016/j.bone.2012.11.005.
24. Ozasa R, Ishimoto T, Miyabe S, *et al*., 2019, Osteoporosis Changes Collagen/Apatite Orientation and Young's Modulus in Vertebral Cortical Bone of Rat. *Calcif Tissue Int*, 104:449–60. DOI: 10.1007/s00223-018-0508-z.
25. Matsugaki A, Harada T, Kimura Y, *et al*., 2018, Dynamic Collision Behavior between Osteoblasts and Tumor Cells Regulates the Disordered Arrangement of Collagen Fiber/Apatite Crystals in Metastasized Bone. *Int J Mol Sci*, 19:3474. DOI: 10.3390/ijms19113474.
26. Zeng J, Matsusaki M, 2019, Layer-by-Layer Assembly of Nanofilms to Control Cell Functions. *Polym Chem*, 10:2960–74. DOI: 10.1039/c9py00305c.
27. Lee S, Matsugaki A, Kasuga T, *et al*., 2019, Development of bifunctional oriented bioactive glass/poly(lactic acid) composite scaffolds to control osteoblast alignment and proliferation. *J Biomed Mater Res A*, 107:1031–41.
28. Ozasa R, Matsugaki A, Isobe Y, *et al*., 2018, Construction of Human Induced Pluripotent Stem Cell-derived Oriented Bone Matrix Microstructure by Using *In Vitro* Engineered Anisotropic Culture Model. *J Biomed Mater Res A*, 106:360–9. DOI: 10.1002/jbm.a.36238.
29. Matsugaki A, Fujiwara N, Nakano T, 2013, Continuous Cyclic Stretch Induces Osteoblast Alignment and Formation of Anisotropic Collagen Fiber Matrix. *Acta Biomater*, 9:7227–35. DOI: 10.1016/j.actbio.2013.03.015.
30. Wang L, Wang Y, Han Y, *et al*., 2005, *In Situ* Measurement of Solute Transport in the Bone Lacunar-canalicular System. *Proc Natl Acad Sci U S A*, 102:11911–6. DOI: 10.1073/pnas.0505193102.
31. Wang J, Ishimoto T, Nakano T, *et al*., 2017, Unloading-induced Degradation of the Anisotropic Arrangement of Collagen/Apatite in Rat Femurs. *Calcif Tissue Int*, 100:87–94. DOI: 10.1007/s00223-016-0200-0.
32. Zhang K, Barragan-Adjemian C, Ye L, *et al*., 2006, E11/gp38 Selective Expression in Osteocytes: Regulation by Mechanical Strain and Role in Dendrite Elongation. *Mol Cell Biol*, 26:4539–52. DOI: 10.1128/mcb.02120-05.
33. Thi MM, Suadicani SO, Schaffler MB, *et al*., 2013, Spray Mechanosensory Responses of Osteocytes to Physiological Forces Occur Along Processes and not Cell Body and Require αVβ3 Integrin. *Proc Natl Acad Sci U S A*, 110:21012–7. DOI: 10.1073/pnas.1321210110.
34. Wang Y, Botvinick L, Zhao Y, *et al*., 2005, Visualizing the Mechanical Activation of SRC. *Nature*, 434:1040–5.
35. Schimmel L, Fukuhara D, Richards M, *et al*., 2020, c-SRC Controls Stability of Sprouting Blood Vessels in the Developing Retina Independently of Cell-cell Adhesion through Focal Adhesion Assembly. *Development*, 147:dev185405. DOI: 10.1242/dev.185405.
36. Skupien A, Konopka A, Trzaskoma P, *et al.*, 2014, CD44 Regulates Dendrite Morphogenesis through SRC Tyrosine Kinase-dependent Positioning of the Golgi. *J Cell Biol*, 127:5038–51. DOI: 10.1242/jcs.154542.